

Axial Donor Effects on Oxidatively Induced Ethane Formation from Nickel–Dimethyl Complexes

Sofia M. Smith,[†] Nigam P. Rath,[§] and Liviu M. Mirica^{*,†,‡}

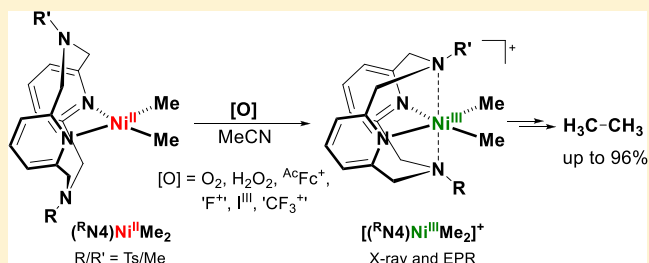
[‡]Department of Chemistry, University of Illinois at Urbana–Champaign, 600 South Mathews Avenue, Urbana, Illinois 61801, United States

[†]Department of Chemistry, Washington University in St. Louis, One Brookings Drive, St. Louis, Missouri 63130-4899, United States

[§]Department of Chemistry and Biochemistry, University of Missouri–St. Louis, One University Boulevard, St. Louis, Missouri 63121-4400, United States

S Supporting Information

ABSTRACT: Tetradentate pyridinophane ligands have been shown to stabilize uncommon high-valent palladium and nickel organometallic complexes. Described herein are the synthesis and detailed characterization of a series of Ni^{II}– and Ni^{III}–dimethyl complexes supported by modified tetradentate pyridinophane ligands in which one or both of the *N*-methyl substituents were replaced with electron-withdrawing *p*-toluenesulfonyl groups, thus reducing the amine *N* atom donicity and favoring the formation of Ni complexes with lower coordination numbers. The corresponding Ni^{II}–dimethyl complexes exhibit accessible oxidation potentials, and their oxidation generates Ni^{III} species that were characterized by EPR and X-ray crystallography. Moreover, the Ni^{II}–dimethyl complexes exhibit selective ethane formation upon oxidatively induced reductive elimination using various oxidants—including O₂ and H₂O₂, without the generation of any C–heteroatom products. Overall, these results suggest that the (R⁴N4)Ni^{II}Me₂ complexes with more weakly donating axial ligands are more reactive toward ethane formation, likely due to destabilization of the corresponding high-valent Ni intermediates and formation of 5- and 4-coordinate conformations for these Ni species.



INTRODUCTION

Palladium and nickel catalysts have been widely employed in C–C and C–heteroatom bond formation reactions, such as Negishi, Kumada, and Suzuki cross-coupling reactions.^{1–10} Pd catalysts are more commonly used in these transformations, in part due to a thorough mechanistic understanding of the Pd-catalyzed reactions that proceed through Pd^{II}/Pd⁰ catalytic cycles. By comparison, the mechanism of Ni-catalyzed cross-coupling reactions is less understood, especially since Ni is more prone to undergoing one-electron redox reactions.^{11–22} In this context, many studies strongly suggest that paramagnetic Ni^{III} species are key intermediates in C–C and C–heteroatom bond formation reactions.^{6–10,22–30}

In the past several years, we have employed tetradentate pyridinophane ligands to stabilize uncommon organometallic Pd^{III/IV} and Ni^{III/IV} complexes^{31–40} and have shown that these high-valent complexes are capable of C–C and/or C–heteroatom bond formation reactions. For example, we have recently reported the use of *N,N'*-dimethyl-2,11-diaza[3.3]-(2,6)pyridinophane (Me⁴N4) ligand to stabilize high-valent Ni^{III} complexes that undergo C–C bond formation reactions.⁴⁰ Herein, we report the use of modified pyridinophane ligands to probe the effect of axial amine donicity on the reactivity of the corresponding Ni–dimethyl complexes. As such, we have replaced one or both of the *N*–Me groups in Me⁴N4 with more

electron-withdrawing and sterically demanding toluenesulfonyl (tosyl, Ts) groups. The oxidatively induced reductive elimination reactivity studies with various oxidants suggest that the less coordinating the axial ligand is, the more reactive (and less stable) is the corresponding high-valent Ni species, thus leading to faster reductive elimination. Among the three systems investigated, the (Ts⁴N4)Ni^{II}Me₂ complex is shown to be the most reactive and generates ethane selectively at low temperatures, even when oxidants such as O₂ or H₂O₂ were employed.

RESULTS AND DISCUSSION

Synthesis and Characterization of Ni^{II/III} Complexes.

The ligands *N,N'*-dimethyl-2,11-diaza[3.3]-(2,6)pyridinophane (Me⁴N4), *N,N'*-tosylmethyl-2,11-diaza[3.3]-(2,6)pyridinophane (TsMe⁴N4), and *N,N'*-ditosyl-2,11-diaza[3.3]-(2,6)pyridinophane (Ts⁴N4) (Chart 1) were synthesized according to a literature procedure.⁴¹ Complexes (Me⁴N4)Ni^{II}Me₂, **1**, and [(Me⁴N4)Ni^{III}Me₂]⁺, **1**⁺, were synthesized as reported previously.⁴⁰

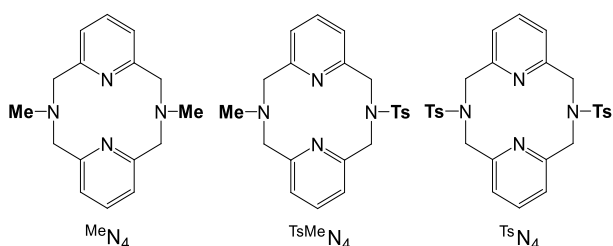
The dark orange complex (TsMe⁴N4)Ni^{II}Me₂, **2**, was prepared in 86% yield from the precursor (TsMe⁴N4)Ni^{II}Br₂ via transmetalation with methylmagnesium chloride (Scheme 1).

Received: June 29, 2019

Published: September 20, 2019



Chart 1. Ligands Used for Stabilizing High-Valent Nickel Complexes



The single crystal X-ray structure of **2** reveals a square planar geometry for the Ni center that is bound to two pyridyl nitrogen atoms from the $^{TsMe}N_4$ ligand and two methyl groups, with an average equatorial Ni–N_{pyridyl} bond length of 1.947 Å and an average Ni–C bond length of 1.929 Å (Figure 1). As expected, **2** is diamagnetic, likely due to the strong σ -donor methyl groups that favor the low-spin square planar geometry, in contrast to the $(^R N_4)Ni^{II}Br_2$ precursors that adopt octahedral geometries. The cyclic voltammogram (CV) of **2** exhibits an oxidation wave at –890 mV vs Fc⁺/Fc (Figure 2) that is tentatively assigned to the Ni^{II/III} redox couple by comparison to the analogous $(^{Me}N_4)Ni^{II}Me_2$ complex **1**,⁴⁰ followed by ill-defined oxidation events at higher potentials.⁴²

Using the same process as described above, we were able to prepare the orange complex $(^{Ts}N_4)Ni^{II}Me_2$, **3**, in 38% yield from the precursor $(^{Ts}N_4)Ni^{II}Br_2$. Similar to **2**, the single crystal X-ray structure of **3** reveals a square planar geometry for the Ni center, with an average equatorial Ni–N_{pyridyl} bond length of 1.974 Å and an average Ni–C bond length of 1.943 Å (Figure 1). Complexes **2** and **3** were both characterized by ¹H and ¹³C NMR.⁴² The CV of **3** exhibits an oxidation process at –430 mV vs Fc⁺/Fc (Figure 2) that is tentatively assigned to the Ni^{II/III} redox couple,⁴⁰ followed by ill-defined oxidation events at higher potentials.⁴² Notably, when comparing the Ni^{II/III} oxidation potentials for **1**,⁴⁰ **2**, and **3**, it seems that these values increase by ~500 mV for every tosyl group that replaces a methyl group as the N-substituent, a trend that was previously observed for similar Pd complexes and was attributed to the interaction of the axial N donors with the metal center.³⁵

Both **2** and **3** can be oxidized using 1 equiv of silver hexafluoroantimonate (AgSbF₆) in THF at –50 °C to generate the species $[(^{TsMe}N_4)Ni^{III}Me_2]SbF_6$, **2**⁺, and $[(^{Ts}N_4)Ni^{III}Me_2]SbF_6$, **3**⁺, respectively. Single crystal X-ray characterization of **2**⁺ reveals a six-coordinate Ni^{III} center in a distorted

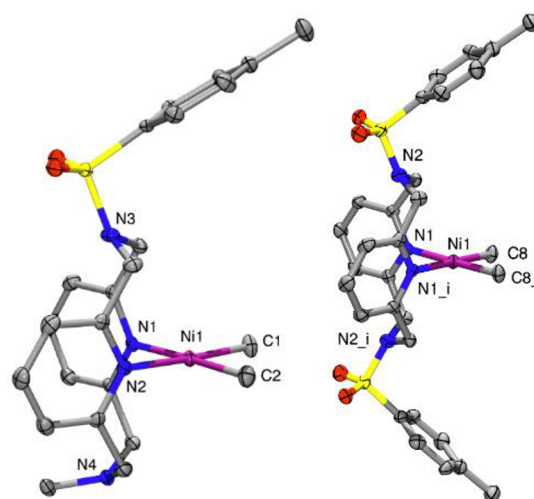
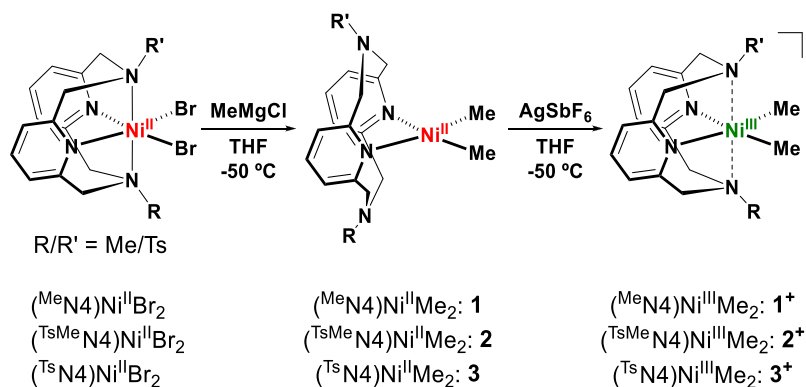


Figure 1. ORTEP representation of **2** (left) and **3** (right), with 50% probability thermal ellipsoids. Selected bond distances (Å): **2**: Ni1–C1, 1.934(11); Ni1–C2, 1.923(12); Ni1–N1, 1.976(8); Ni1–N2, 1.971(9). **3**: Ni1–C8, 1.929(4); Ni1–C8i, 1.929(4); Ni1–N1, 1.974(3); Ni1–N1i, 1.974(3).

octahedral geometry, with the average equatorial Ni–N_{pyridyl} bond lengths being similar to the previously reported organometallic $(^R N_4)Ni^{III}$ complexes,^{39,40} while the axial Ni–N_{Ts} distance (2.456 Å) is longer than the Ni–N_{Me} distance of 2.154(11) Å (Figure 3), due to the more electron deficient nature of the tosyl group that weakens the donicity of the N donor, as well as the stronger *trans* influence of the N_{Me} group. Moreover, the 2.154(11) Å Ni–N_{Me} distance in **2**⁺ is shorter than the average Ni–N_{Me} distance of 2.246 Å of $[(^{Me}N_4)Ni^{III}Me_2]$, **1**⁺.⁴⁰ While a Ni–N_{Ts} interaction is present in the solid-state structure, it is possible that **2**⁺ adopts a 5-coordinate geometry in solution (vide infra). Finally, despite several attempts, we were not able to obtain X-ray quality crystals for complex **3**⁺ due to its limited stability.

The EPR spectrum of **2**⁺ reveals a pseudoaxial signal in THF:2-methyl-THF (MeTHF), and superhyperfine coupling to the two axial N donors (*I* = 1) was observed in the *g_z* direction (Figure 4). The optimal simulation of the EPR spectrum was obtained when different coupling constants were used for the axial N_{Me} (*A_z* = 17.5 G) and N_{Ts} donors (*A_z* = 6 G), and the values are in line with the stronger Ni–N_{Me} vs Ni–N_{Ts} interaction observed by X-ray crystallography and consistent with the more electron-withdrawing nature of the

Scheme 1. Synthesis of $(^R N_4)NiMe_2$ Complexes

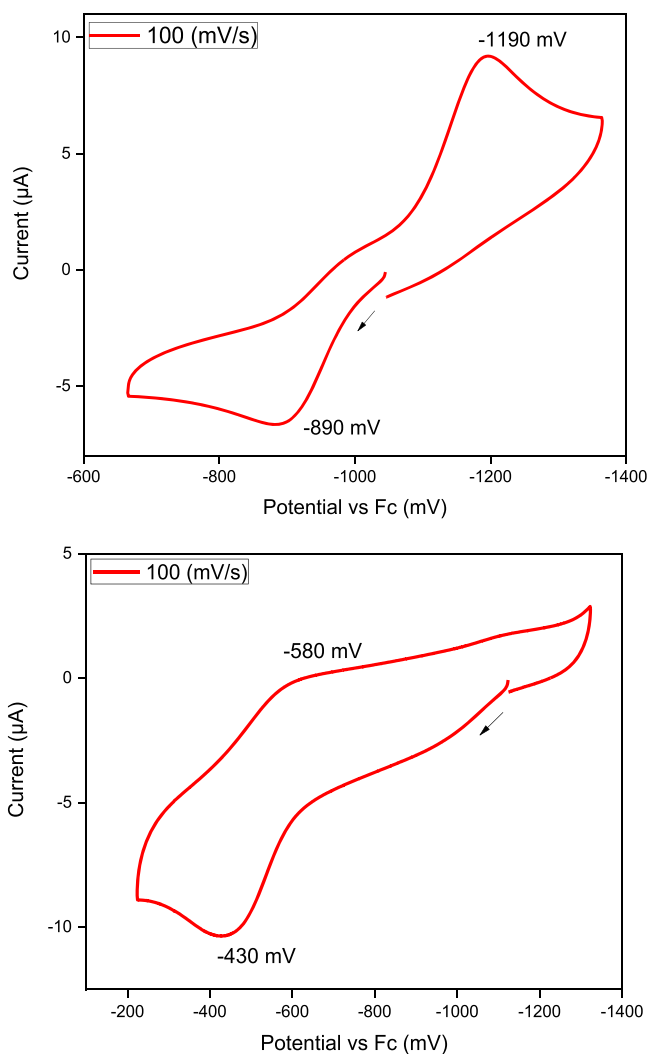


Figure 2. CV of **2** (top) in 0.1 M $n\text{Bu}_4\text{NPF}_6/\text{MeCN}$ at RT (100 mV/s scan rate) and CV of **3** (bottom) in 0.1 M $n\text{Bu}_4\text{NPF}_6/\text{MeCN}$ at RT (100 mV/s scan rate).

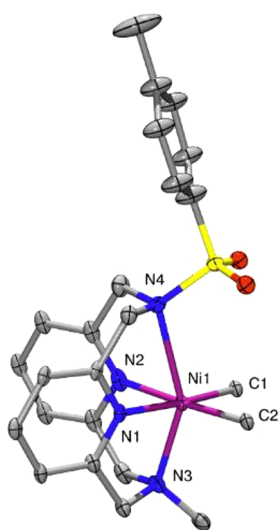


Figure 3. ORTEP representation of 2^+ with 50% probability thermal ellipsoids. Selected bond distances (Å), 2^+ : Ni1–C1, 1.932(3); Ni1–C2, 1.925(3); Ni1–N1, 1.968(2); Ni1–N2, 1.965(2); Ni1–N3, 2.154(11); Ni1–N4, 2.456.

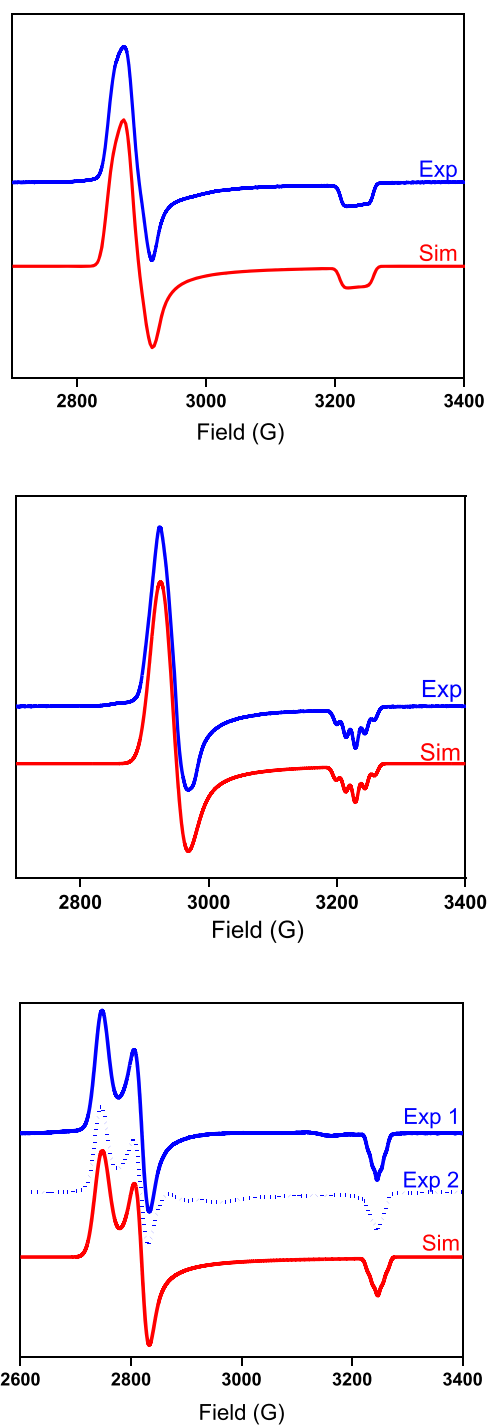


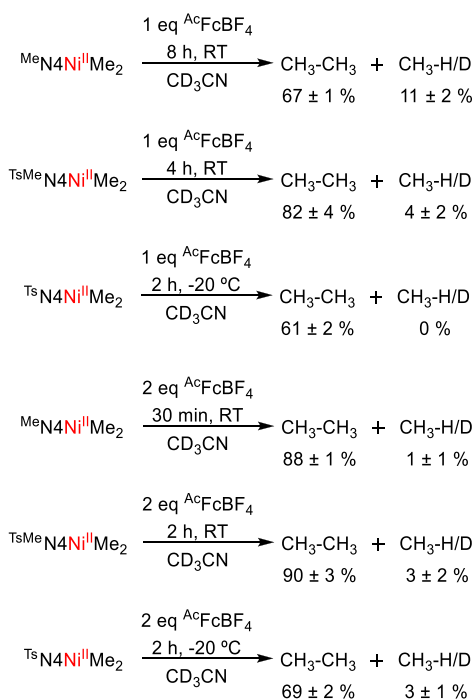
Figure 4. Top: experimental (1:3 THF:MeTHF, 77 K) and simulated EPR spectra of 2^+ using the following parameters: $g_x = 2.270$ ($A_x = 12.0$ G), $g_y = 2.243$ ($A_y = 12.0$ G), $g_z = 2.011$ ($A_z(\text{N}) = 17.5$ G and $A_z(\text{N}) = 6$ G). Center: experimental (1:3 MeCN:PrCN, 77 K) and simulated EPR spectra of 2^+ using the following parameters: $g_x = 2.222$, $g_y = 2.202$, $g_z = 2.012$ ($A_z(2\text{N}) = 15.0$ G). Bottom: experimental (1:3 MeCN:PrCN, blue line, and 1:3 THF:MeTHF, blue dashed line, 77 K) and simulated EPR spectra of 3^+ using the following parameters: $g_x = 2.365$, $g_y = 2.304$, $g_z = 2.002$ ($A_z(2\text{N}) = 9.0$ G).

tosyl group, as well as the stronger *trans* influence of the N_{Me} donor. Interestingly, when the EPR spectrum of 2^+ was obtained in MeCN:PrCN, the signal was best simulated using superhyperfine coupling to the two axial N donors with

identical coupling constants ($A_z = 15.0$ G) and giving rise to a quintet with a 1:2:3:2:1 intensity ratio,⁴² suggesting that a solvent molecule (MeCN or PrCN) replaced the N_{T_s} axial ligand and interacts with the Ni center. By comparison, the EPR spectrum of 3^+ in MeCN:PrCN shows a rhombic signal with weak superhyperfine coupling ($A_z = 9.0$ G) in the g_z region to two N atoms (Figure 4). Since the EPR spectrum of 3^+ in THF:MeTHF is similar to the one obtained in MeCN:PrCN (although 3^+ is less stable in the former solvent mixture, likely due to a more exposed Ni^{III} center), we propose that the observed weak coupling in the g_z region should correspond to the weakly interacting axial ligands, either the N_{T_s} donors or the nitrile solvent molecules.⁴²

C–C Bond Formation Reactivity of $(^R N_4)Ni^{II}Me_2$ Complexes. The organometallic reactivity of **1**, **2**, and **3** was investigated and compared under different reaction conditions. First, the oxidatively induced reductive elimination from **1**, **2**, or **3** in CD_3CN was probed using $^{Ac}FcBF_4$ as an outer-sphere oxidant, and the yields of ethane (and methane as side product) were monitored via 1H NMR over time until the reaction was complete (Scheme 2 and Table 1),⁴² the

Scheme 2. C–C Bond Formation Reactivity of the $(^R N_4)Ni^{II}Me_2$ Complexes with $^{Ac}FcBF_4$

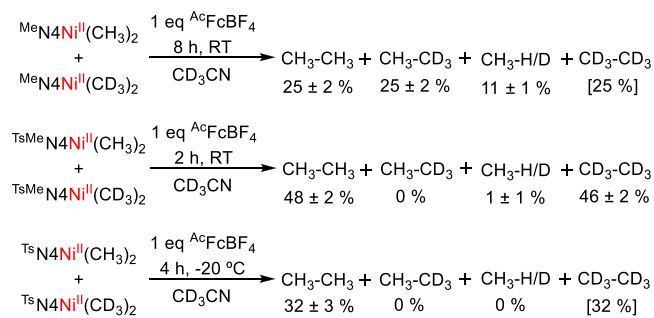


formation of methane is proposed to occur upon hydrogen atom abstraction from the solvent or ligand molecules by the methyl radicals generated upon homolysis of Ni–Me bonds.^{38,40} When 1 equiv of $^{Ac}FcBF_4$ was added to MeCN solutions of **1**, **2**, and **3**, a general trend was observed in which complexes **2** and **3** supported by the $^R N_4$ ligands with the more electron-withdrawing N-substituents yielded higher yields of ethane, while the formation of methane was also minimized for ligands bearing tosyl groups.⁴⁰ Complex **2** gave the highest yield of ethane (82%), while the TsN_4 complex **3** gave ethane in 61% yield; however, the reaction had to be performed at $-20^\circ C$ for the latter system to prevent the formation of Ni^0 . Interestingly, addition of 2 equiv of $^{Ac}FcBF_4$ to solutions of **1**, **2**, or **3** increased the yield of ethane and

decreased the yield of methane (Scheme 2). The most pronounced difference was observed for **1**, which gave ethane in 88% yield after only 30 min at RT. This result is similar to what was observed previously, and this was proposed to be due to a change in the mechanism of C–C bond formation that will likely involve a Ni^{IV} intermediate upon two-electron oxidation.⁴⁰ By comparison, for complexes **2** and **3**, the yield of ethane increased only slightly to 90 and 69%, respectively.⁴² Overall, these results suggest a more facile oxidatively induced C–C reductive elimination for the $NiMe_2$ complexes supported by the $^R N_4$ ligands containing N_{T_s} donors, which only weakly interact axially with the Ni center. Such weak interactions destabilize the corresponding Ni^{III} species, as described above, and decoordination of the N_{T_s} donors would allow the formation of 5- and 4-coordinate geometries that should rapidly undergo reductive elimination. As such, the $TsMeN_4$ ligand provides the optimal effect of supporting a Ni^{III} species while also allowing for rapid and selective ethane elimination.

Additional mechanistic studies were performed to probe the observed C–C bond formation reactivity for complexes **1**, **2**, and **3**. Crossover experiments using a 1:1 mixture of $(^R N_4)Ni^{II}Me_2$ and $(^R N_4)Ni^{II}(CD_3)_2$ in CD_3CN revealed two types of results upon addition of 1 equiv of $^{Ac}FcBF_4$. As observed previously for complex **1**, a 1:1 mixture of CH_3CH_3 and CH_3CD_3 was generated in $\sim 25\%$ yield for each product after 8 h (Scheme 3), which suggests a methyl group transfer

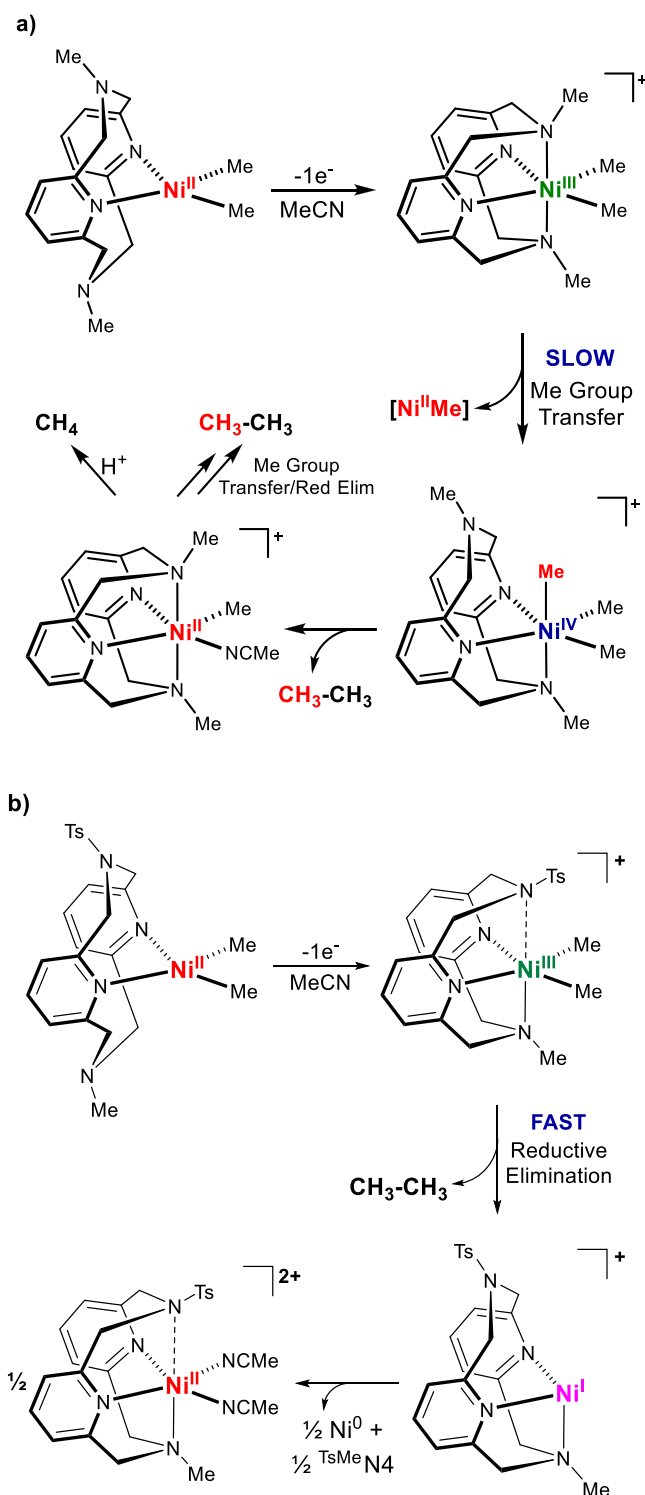
Scheme 3. Crossover Reactivity Studies of the $(^R N_4)Ni^{II}Me_2$ Complexes



involving two Ni centers, followed by a rapid rearrangement of the methyl groups between the axial and equatorial positions before the reductive elimination step (Scheme 4a).⁴⁰ By comparison, for either mixture of **2:2-d6** or **3:3-d6**, no crossover product CH_3CD_3 was observed, with CH_3CH_3 being formed in 48 and 32% yield, respectively. The formation of an equivalent amount of CD_3CD_3 (46% yield) was also confirmed by 2H NMR for the reaction of the **2:2-d6** mixture. Moreover, a similar distribution of products was observed when 2 equiv of $^{Ac}FcBF_4$ was used for the oxidation of either mixture of **2:2-d6** or **3:3-d6**.⁴²

On the basis of these reactivity studies, we propose that complexes **2** and **3** proceed through a different oxidatively induced C–C bond formation mechanism than complex **1** (Scheme 4).⁴⁰ It is likely that, upon one-electron oxidation of the Ni^{II} complexes **2** and **3**, the generation of Ni^{III} species that adopt 5- or 4-coordinate geometries leads to fast intramolecular reductive elimination to generate ethane and a Ni^I species (Scheme 4b). This Ni^I species can then undergo disproportionation to form a $(^R N_4)Ni^{II}$ –solvento complex,⁴²

Scheme 4. (a) Previously Reported Mechanism for the Oxidatively Induced Ethane Formation from $(^{\text{Me}}\text{N4})\text{Ni}^{\text{II}}\text{Me}_2$, **1**,^a and (b) Proposed Mechanism for Oxidatively Induced Ethane Formation from $(^{\text{TsMe}}\text{N4})\text{Ni}^{\text{II}}\text{Me}_2$, **2**^b



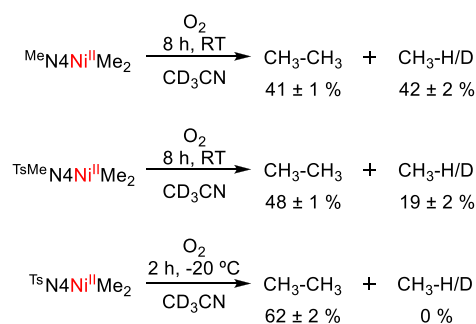
^aThe methyl groups marked in red are meant to represent isotopic labeling.⁴⁰ ^bA similar mechanism could be envisioned for $(^{\text{Ts}}\text{N4})\text{Ni}^{\text{II}}\text{Me}_2$ (**3**).

free ligand, and Ni^0 , which were isolated or observed at the end of the reaction. By comparison, oxidation by one electron of

complex **1** generates a more stable 6-coordinate Ni^{III} species, followed by a subsequent methyl group transfer between two Ni centers to generate a transient $(^{\text{RN4}}\text{Ni}^{\text{IV}}\text{Me}_3$ species that will undergo reductive elimination to yield ethane, including the crossover product CH_3CD_3 (Scheme 4a). Moreover, since complex **1** exhibits a $\text{Ni}^{\text{III/IV}}$ oxidation potential at ~ 0 mV vs Fc/Fc^+ , addition of 2 equiv of $^{\text{Ac}}\text{FcBF}_4$ (with an oxidation potential of ~ 250 mV vs Fc/Fc^+) is expected to generate a transient Ni^{IV} species that directly eliminates ethane, without the need for methyl group transfer.⁴⁰ Since for **2** and **3** the Ni^{IV} oxidation state is not easily accessible due to the weak donating ability of the axial N_{Ts} donors,⁴² addition of 2 equiv of $^{\text{Ac}}\text{FcBF}_4$ should not change the mechanism of ethane elimination. Finally, as we have shown previously for both $(^{\text{RN4}}\text{Pd})\text{Me}_2$ and $(^{\text{RN4}}\text{Ni})\text{Me}_2$ complexes,^{35,38,40} the ethane elimination reactivity is similar when other outer-sphere oxidants with comparable oxidation potentials were employed.

We have also probed alternate oxidants, including ones that could proceed through an inner sphere mechanism, to compare the C–C vs C–heteroatom bond formation reactivity. Excitingly, complexes **1**, **2**, and **3** can be readily oxidized with oxidants such as O_2 or H_2O_2 to generate ethane in yields up to 70% (Scheme 5 and Table 1), while no C–O

Scheme 5. C–C Bond Formation Reactivity of the $(^{\text{RN4}}\text{Ni}^{\text{II}}\text{Me}_2$ Complexes with O_2



products were observed for any of these complexes. Interestingly, in the presence of O_2 , the yield of ethane increases from **1** to **2** to **3**, while the yield of the side product methane decreases in the same direction, further suggesting that the presence of N-Ts substituents in the $^{\text{RN4}}$ ligands promotes more facile C–C bond formation reactivity. Thus, even though complex **3** exhibits a $\text{Ni}^{\text{II}}/\text{Ni}^{\text{III}}$ redox potential at -505 mV vs Fc^+/Fc , it can rapidly react with O_2 or H_2O_2 to selectively generate ethane. In addition, complexes **1**, **2**, and **3** can also react with other oxidants such as 1-fluoro-2,4,6-trimethylpyridinium triflate (NFTPT), (diacetoxyiodo)benzene, and 5-(trifluoromethyl)dibenzothiophenium trifluoromethanesulfonate (TDTT) to generate ethane in up to 96% yield, with no C–F, C–O, or C–CF₃ bond formation products being observed in any of these cases (Table 1).⁴² The same trend was observed for these oxidants, with a higher yield of ethane being obtained for **3** over **2** over **1**. This trend parallels the decrease in stability of the corresponding Ni^{III} species and does not seem to correlate with the oxidation potential or the outer-sphere/inner-sphere nature of the oxidant employed. Overall, these oxidatively induced ethane formation reactions confirm that employing $^{\text{RN4}}$ ligands that contain electron-withdrawing tosyl N-substituents promotes more facile C–C reductive elimination from Ni centers. Compared with the

Table 1. Oxidatively Induced Reactivity of Complexes 1, 2, and 3

oxidant ^a	^{(Me)N4} Ni ^{III} Me ₂ (1)		^(^{TsMe}N4) Ni ^{III} Me ₂ (2)		^(^{Ts}N4) Ni ^{III} Me ₂ (3) ^b	
	CH ₃ –CH ₃ (%)	CH ₃ –H/D (%)	CH ₃ –CH ₃ (%)	CH ₃ –H/D (%)	CH ₃ –CH ₃ (%)	CH ₃ –H/D (%)
1 equiv of ^{Ac} FcBF ₄	67 ± 1	11 ± 2	82 ± 4	4 ± 2	61 ± 2	0
2 equiv of ^{Ac} FcBF ₄	88 ± 1 ^c	1 ± 1	90 ± 3	3 ± 2	69 ± 1	3 ± 1
O ₂	41 ± 1	42 ± 2	48 ± 1	19 ± 2	62 ± 2	0
H ₂ O ₂	69 ± 3	7 ± 2	70 ± 1	13 ± 1	61 ± 1	0
NFTPT	49 ± 3	9 ± 2	87 ± 1	6 ± 1	96 ± 1	0
PhI(OAc) ₂	74 ± 2	11 ± 1	85 ± 1	6 ± 2	88 ± 2	8 ± 1
TDDT	79 ± 1	20 ± 2	86 ± 2	13 ± 1	88 ± 1	0

^aTypical reaction conditions: MeCN, RT, 2–8 h. ^bReactions performed at –20 °C. ^c30 min.

^{Me}N4 ligand, which stabilizes to a greater extent Ni^{III} centers and even Ni^{IV} species, the ^{TsMe}N4 and especially the ^{Ts}N4 ligand are proposed to destabilize the high-valent Ni species due to the weaker axial Ni–N_{Ts} interactions, while allowing for the formation of 5- and 4-coordinate conformations that can rapidly undergo reductive elimination. Importantly, all of the (^RN4)NiMe₂ complexes described herein react with a range of oxidants, including O₂ and H₂O₂, to cleanly generate ethane and without the formation of any C–heteroatom bond formation products.

Catalytic Reactivity of (^RN4)Ni^{II}Br₂ Complexes. In addition to stoichiometric C–C and C–X bond formation studies, we also investigated the ability of the precursor (^RN4)NiBr₂ complexes to catalyze the Kumada cross-coupling reaction. Indeed, these complexes are efficient catalysts for the coupling of aryl iodides with aryl Grignard reagents, with (^{TsMe}N4)NiBr₂ being the optimal catalyst to generate the aryl–aryl coupled product in 94% yield (Table 2).⁴² However, these

Table 2. Kumada Cross-Coupling Reactions Catalyzed by (^RN4)Ni^{II}Br₂

R–X + R'–MgBr		$\xrightarrow[\text{THE, RT, 2h}]{5\text{mol}\% (\text{R}^{\text{N4}})\text{Ni}^{\text{II}}\text{Br}_2}$ R–R'		
		ligand ^a		
R–X	R' MgX	^{Me} N4	^{TsMe} N4	^{Ts} N4
<i>p</i> -tolyl-I	PhMgBr	80 ± 2	95 ± 2	60 ± 2
<i>p</i> -tolyl-I	hexylMgBr	36 ± 1	38 ± 2	17 ± 2
octyl-I	PhMgBr	14 ± 2	15 ± 2	5 ± 1

^aYields (%) were determined by GC-FID vs decane as internal standard; no coupled products were observed in these reactions in the absence of (^RN4)NiBr₂.

catalysts gave only modest yields for the coupling of aryl iodides with alkyl Grignard reagents or alkyl iodides with aryl Grignard reagents. While these results are not outstanding, they do suggest that the (^RN4)Ni complexes described herein are relevant to classical cross-coupling reactions, which are commonly proposed to involve Ni^{III} transient intermediates.^{7,8,24,25} As we have shown previously, the reaction of (^RN4)Ni complexes with Grignard reagents and aryl/alkyl halides generates in situ detectable Ni^{III} species, which are responsible for C–C bond formation upon reductive elimination.³⁴

CONCLUSION

In conclusion, we report herein the use of three pyridinophane ^RN4 ligands with either methyl or electron-withdrawing tosyl N-substituents to synthesize a series of (^RN4)NiMe₂

complexes and investigate their oxidatively induced C–C and C–heteroatom bond formation reactivity. The (^RN4)–Ni^{II}Me₂ complexes can be oxidized with a mild oxidant to generate [(^RN4)Ni^{III}Me₂]⁺ species that were characterized by X-ray crystallography or EPR spectroscopy. Moreover, these Ni^{II}–dimethyl complexes exhibit selective ethane formation upon oxidatively induced reductive elimination using various oxidants, including O₂ and H₂O₂, without the formation of any C–heteroatom bond formation products. Compared with the ^{Me}N4 ligand, which stabilizes to a greater extent the Ni^{III} centers and even Ni^{IV} species, the ^{TsMe}N4 and ^{Ts}N4 ligands are proposed to destabilize the high-valent Ni species due to the weaker axial Ni–N_{Ts} interactions, while allowing for the formation of 5- and 4-coordinate conformations that can rapidly undergo reductive elimination.

ASSOCIATED CONTENT

Supporting Information

The Supporting Information is available free of charge on the ACS Publications website at DOI: 10.1021/acs.organomet.9b00438.

Synthetic details, spectroscopic characterization, stoichiometric and catalytic reactivity studies, and crystallographic data (PDF)

Accession Codes

CCDC 1895832–1895834 and 1895836–1895837 contain the supplementary crystallographic data for this paper. These data can be obtained free of charge via www.ccdc.cam.ac.uk/data_request/cif, or by emailing data_request@ccdc.cam.ac.uk, or by contacting The Cambridge Crystallographic Data Centre, 12 Union Road, Cambridge CB2 1EZ, UK; fax: +44 1223 336033.

AUTHOR INFORMATION

Corresponding Author

*E-mail: mirica@illinois.edu.

ORCID

Sofia M. Smith: 0000-0002-7005-4034

Liviu M. Mirica: 0000-0003-0584-9508

Notes

The authors declare no competing financial interest.

ACKNOWLEDGMENTS

We thank the National Science Foundation (NSF CHE-1255424 and CHE-1925751) for support. The purchase of the Bruker EMX-PLUS EPR spectrometer was supported by the National Science Foundation (MRI, CHE-1429711). We also thank Dr. Jason W. Schultz for the EPR measurements.

REFERENCES

- (1) Diederich, F.; Stang, P. J. *Metal-Catalyzed Cross-Coupling Reactions*; Wiley-VCH: Weinheim, Germany; New York, 1998.
- (2) Terao, J.; Kambe, N. Cross-Coupling Reaction of Alkyl Halides with Grignard Reagents Catalyzed by Ni, Pd, or Cu Complexes with pi-Carbon Ligand(s). *Acc. Chem. Res.* **2008**, *41* (11), 1545–1554.
- (3) Glorius, F. Asymmetric Cross-Coupling of Non-Activated Secondary Alkyl Halides. *Angew. Chem., Int. Ed.* **2008**, *47* (44), 8347–8349.
- (4) Hartwig, J. F. *Organotransition Metal Chemistry: From Bonding to Catalysis*; University Science Books: Sausalito, CA, 2010; p 1127.
- (5) Vabre, B.; Spasyuk, D. M.; Zargarian, D. Impact of Backbone Substituents on POCOP-Ni Pincer Complexes: A Structural, Spectroscopic, and Electrochemical Study. *Organometallics* **2012**, *31* (24), 8561–8570.
- (6) Frisch, A. C.; Beller, M. Catalysts for cross-coupling reactions with non-activated alkyl halides. *Angew. Chem., Int. Ed.* **2005**, *44* (5), 674–688.
- (7) Phapale, V. B.; Cardenas, D. J. Nickel-catalyzed Negishi cross-coupling reactions: scope and mechanisms. *Chem. Soc. Rev.* **2009**, *38* (6), 1598–1607.
- (8) Netherton, M. R.; Fu, G. C. Nickel-catalyzed cross-couplings of unactivated alkyl halides and pseudohalides with organometallic compounds. *Adv. Synth. Catal.* **2004**, *346* (13–15), 1525–1532.
- (9) Rudolph, A.; Lautens, M. Secondary Alkyl Halides in Transition-Metal-Catalyzed Cross-Coupling Reactions. *Angew. Chem., Int. Ed.* **2009**, *48* (15), 2656–2670.
- (10) Knochel, P.; Thaler, T.; Diene, C. Pd-, Ni-, Fe-, and Co-Catalyzed Cross-Couplings Using Functionalized Zn-, Mg-, Fe-, and In-Organometallics. *Isr. J. Chem.* **2010**, *50* (5–6), 547–557.
- (11) Amatore, C.; Jutand, A. Rates and mechanism of biphenyl synthesis catalyzed by electrogenerated coordinatively unsaturated nickel complexes. *Organometallics* **1988**, *7* (10), 2203–14.
- (12) Tsou, T. T.; Kochi, J. K. Reductive Coupling of Organometals Induced by Oxidation - Detection of Metastable Paramagnetic Intermediates. *J. Am. Chem. Soc.* **1978**, *100* (5), 1634–1635.
- (13) Koo, K. M.; Hillhouse, G. L.; Rheingold, A. L. Oxygen-Atom Transfer from Nitrous-Oxide to an Organonickel(II) Phosphine Complex - Syntheses and Reactions of New Nickel(II) Aryloxides and the Crystal-Structure of (Me(2)Pch(2)Ch(2)Pme(2))Ni(O-O-C(6)-H(4)Cme(2)Ch(2)). *Organometallics* **1995**, *14* (1), 456–460.
- (14) Han, R. Y.; Hillhouse, G. L. Carbon-oxygen reductive-elimination from nickel(II) oxametallacycles and factors that control formation of ether, aldehyde, alcohol, or ester products. *J. Am. Chem. Soc.* **1997**, *119* (34), 8135–8136.
- (15) Matsunaga, P. T.; Mavropoulos, J. C.; Hillhouse, G. L. Oxygen-Atom Transfer from Nitrous-Oxide (N = O=O) to Nickel Alkyls - Syntheses and Reactions to Nickel(II) Alkoxides. *Polyhedron* **1995**, *14* (1), 175–185.
- (16) Lin, B. L.; Clough, C. R.; Hillhouse, G. L. Interactions of aziridines with nickel complexes: Oxidative-addition and reductive-elimination reactions that break and make C-N bonds. *J. Am. Chem. Soc.* **2002**, *124* (12), 2890–2891.
- (17) Yu, S.; Dudkina, Y.; Wang, H.; Kholin, K. V.; Kadirov, M. K.; Budnikova, Y. H.; Vivic, D. A. Accessing perfluoroalkyl nickel(ii), (iii), and (iv) complexes bearing a readily attached [C4F8] ligand. *Dalton Trans* **2015**, *44* (45), 19443–19446.
- (18) Iluc, V. M.; Miller, A. J. M.; Anderson, J. S.; Monreal, M. J.; Mehn, M. P.; Hillhouse, G. L. Synthesis and Characterization of Three-Coordinate Ni(III)-Imide Complexes. *J. Am. Chem. Soc.* **2011**, *133* (33), 13055–13063.
- (19) Klein, A.; Budnikova, Y. H.; Sinyashin, O. G. Electron transfer in organonickel complexes of α -diimines: Versatile redox catalysts for C–C or C–P coupling reactions – A review. *J. Organomet. Chem.* **2007**, *692* (15), 3156–3166.
- (20) Cloutier, J. P.; Zargarian, D. Functionalization of the Aryl Moiety in the Pincer Complex (NCN)(NiBr₂)-Br-III: Insights on Ni-III-Promoted Carbon-Heteroatom Coupling. *Organometallics* **2018**, *37* (9), 1446–1455.
- (21) Spasyuk, D. M.; Zargarian, D.; van der Est, A. New POCN-Type Pincer Complexes of Nickel(II) and Nickel(III). *Organometallics* **2009**, *28* (22), 6531–6540.
- (22) Tsou, T. T.; Kochi, J. K. Mechanism of biaryl synthesis with nickel complexes. *J. Am. Chem. Soc.* **1979**, *101* (25), 7547–60.
- (23) Biswas, S.; Weix, D. J. Mechanism and Selectivity in Nickel-Catalyzed Cross- Electrophile Coupling of Aryl Halides with Alkyl Halides. *J. Am. Chem. Soc.* **2013**, *135*, 16192–16197.
- (24) Hu, X. Nickel-catalyzed cross coupling of non-activated alkyl halides: a mechanistic perspective. *Chem. Sci.* **2011**, *2* (10), 1867–1886.
- (25) Tasker, S. Z.; Standley, E. A.; Jamison, T. F. Recent advances in homogeneous nickel catalysis. *Nature* **2014**, *510* (7503), 176.
- (26) Cornella, J.; Edwards, J. T.; Qin, T.; Kawamura, S.; Wang, J.; Pan, C. M.; Gianatassio, R.; Schmidt, M.; Eastgate, M. D.; Baran, P. S. Practical Ni-Catalyzed Aryl-Alkyl Cross-Coupling of Secondary Redox-Active Esters. *J. Am. Chem. Soc.* **2016**, *138* (7), 2174–2177.
- (27) Cloutier, J. P.; Vabre, B.; Moungang-Soume, B.; Zargarian, D. Synthesis and Reactivities of New NCN-Type Pincer Complexes of Nickel. *Organometallics* **2015**, *34* (1), 133–145.
- (28) Jones, G. D.; Martin, J. L.; McFarland, C.; Allen, O. R.; Hall, R. E.; Haley, A. D.; Brandon, R. J.; Konovalova, T.; Desrochers, P. J.; Pulay, P.; Vivic, D. A. Ligand redox effects in the synthesis, electronic structure, and reactivity of an alkyl-alkyl cross-coupling catalyst. *J. Am. Chem. Soc.* **2006**, *128* (40), 13175–13183.
- (29) Corona, T.; Pfaff, F. F.; Acuna-Pares, F.; Draksharapu, A.; Whiteoak, C. J.; Martin-Diaconescu, V.; Lloret-Fillol, J.; Browne, W. R.; Ray, K.; Company, A. Reactivity of a Nickel(II) Bis(amidate) Complex with meta-Chloroperbenzoic Acid: Formation of a Potent Oxidizing Species. *Chem. - Eur. J.* **2015**, *21* (42), 15029–15038.
- (30) Bour, J. R.; Camasso, N. M.; Meucci, E. A.; Kampf, J. W.; Canty, A. J.; Sanford, M. S. Carbon–Carbon Bond-Forming Reductive Elimination from Isolated Nickel(III) Complexes. *J. Am. Chem. Soc.* **2016**, *138* (49), 16105–16111.
- (31) Khusnutdinova, J. R.; Rath, N. P.; Mirica, L. M. Stable Mononuclear Organometallic Pd(III) Complexes and Their C-C Bond Formation Reactivity. *J. Am. Chem. Soc.* **2010**, *132* (21), 7303–7305.
- (32) Khusnutdinova, J. R.; Rath, N. P.; Mirica, L. M. Dinuclear Palladium(III) Complexes with a Single Unsupported Bridging Halide Ligand: Reversible Formation from Mononuclear Palladium(II) or Palladium(IV) Precursors. *Angew. Chem., Int. Ed.* **2011**, *50* (24), 5532–5536.
- (33) Tang, F. Z.; Zhang, Y.; Rath, N. P.; Mirica, L. M. Detection of Pd(III) and Pd(IV) Intermediates during the Aerobic Oxidative C-C Bond Formation from a Pd(II) Dimethyl Complex. *Organometallics* **2012**, *31* (18), 6690–6696.
- (34) Zheng, B.; Tang, F.; Luo, J.; Schultz, J. W.; Rath, N. P.; Mirica, L. M. Organometallic Nickel(III) Complexes Relevant to Cross-Coupling and Carbon-Heteroatom Bond Formation Reactions. *J. Am. Chem. Soc.* **2014**, *136* (17), 6499–6504.
- (35) Khusnutdinova, J. R.; Rath, N. P.; Mirica, L. M. The Conformational Flexibility of the Tetradentate Ligand tBuN₄ is Essential for the Stabilization of (tBuN₄)Pd(III) Complexes. *Inorg. Chem.* **2014**, *53* (24), 13112–13129.
- (36) Qu, F.; Khusnutdinova, J. R.; Rath, N. P.; Mirica, L. M. Dioxygen activation by an organometallic Pd(II) precursor: formation of a Pd(IV)-OH complex and its C-O bond formation reactivity. *Chem. Commun.* **2014**, *50* (23), 3036–3039.
- (37) Tang, F.; Qu, F.; Khusnutdinova, J. R.; Rath, N. P.; Mirica, L. M. Structural and Reactivity Comparison of Analogous Organometallic Pd(III) and Pd(IV) Complexes. *Dalton Trans* **2012**, *41* (46), 14046–14050.
- (38) Khusnutdinova, J. R.; Rath, N. P.; Mirica, L. M. The Aerobic Oxidation of a Pd(II) Dimethyl Complex Leads to Selective Ethane Elimination from a Pd(III) Intermediate. *J. Am. Chem. Soc.* **2012**, *134*, 2414–2422.

(39) Tang, F. Z.; Rath, N. P.; Mirica, L. M. Stable bis-(trifluoromethyl)nickel(III) complexes. *Chem. Commun.* **2015**, *51* (15), 3113–3116.

(40) Schultz, J. W.; Fuchigami, K.; Zheng, B.; Rath, N. P.; Mirica, L. M. Isolated Organometallic Nickel(III) and Nickel(IV) Complexes Relevant to Carbon-Carbon Bond Formation Reactions. *J. Am. Chem. Soc.* **2016**, *138* (39), 12928–12934.

(41) Wessel, A. J.; Schultz, J. W.; Tang, F.; Duan, H.; Mirica, L. M. Improved synthesis of symmetrically & asymmetrically N-substituted pyridinophane derivatives. *Org. Biomol. Chem.* **2017**, *15* (46), 9923–9931.

(42) See the [Supporting Information](#).